Biophysical Chemistry 158 (2011) 119–125

Contents lists available at ScienceDirect

Biophysical Chemistry

journal homepage: http://www.elsevier.com/locate/biophyschem

Atomic force microscopy analysis of rat pulmonary surfactant films

Xiujun Jiao [a], Eleonora Keating [a], Seyed Tadayyon [b], Fred Possmayer [c,d], Yi Y. Zuo [g], Ruud A.W. Veldhuizen [a,e,f,*]

[a] Lawson Health Research Institute, University of Western Ontario, London, Ontario, Canada
[b] Departments of Chemistry, University of Western Ontario, London, Ontario, Canada
[c] Departments of Obstetrics & Gyneacology, University of Western Ontario, London, Ontario, Canada
[d] Departments of Biochemistry, University of Western Ontario, London, Ontario, Canada
[e] Departments of Medicine, University of Western Ontario, London, Ontario, Canada
[f] Departments of Physiology & Pharmacology, University of Western Ontario, London, Ontario, Canada
[g] Department of Mechanical Engineering, University of Hawaii at Manoa, Honolulu, HI, USA

ARTICLE INFO

Article history:
Received 25 April 2011
Received in revised form 3 June 2011
Accepted 4 June 2011
Available online 13 June 2011

Keywords:
Phospholipid
Cholesterol
Surface pressure-area isotherm
Endogenous surfactant
Phase separation
Langmuir–Wilhelmy surface balance

ABSTRACT

Pulmonary surfactant facilitates breathing by forming a surface tension reducing film at the air–liquid interface of the alveoli. The objective was to characterize the structure of surfactant films using endogenous rat surfactant. Solid-support surfactant films, at different surface pressures, were obtained using a Langmuir balance and were analyzed using atomic force microscopy. The results showed a lipid film structure with three distinct phases: liquid expanded, liquid ordered and liquid condensed. The area covered by the liquid condensed domains increased as surface pressure increased. The presence of liquid ordered phase within these structures correlated with the cholesterol content. At a surface pressure of 50 mN/m, stacks of bilayers appeared. Several structural details of these films differ from previous observations made with goat and exogenous surfactants. Overall, the data indicate that surfactant films demonstrate phase separation at low surface pressures and multilayer formation at higher pressure, features likely important for normal surfactant function.

1. Introduction

The pulmonary surfactant system is essential for normal lung function. By changing the surface tension at the air–liquid interface during the respiratory cycle, surfactant stabilizes the lung and facilitates inflation [1,2]. The prototypic disease in which this important role is evident is neonatal respiratory distress syndrome (NRDS) where surfactant deficiency is the primary cause of lung dysfunction [3]. Administration of exogenous surfactant to the premature lungs of these infants significantly improves lung function and has decreased the mortality associated with NRDS [3]. Abundant evidence indicates that surfactant alterations contribute to decreased lung compliance and low blood oxygenation in other diseases such as acute lung injury (ALI), ventilator associated lung injury, and lung transplantation [4–6]. Roles for surfactant dysfunction have also been described in cystic fibrosis, asthma, alveolar proteinosis, sarcoidosis, idiopathic pulmonary fibrosis and other conditions (reviewed in [7]). A fuller mechanistic understanding of surfactant's biophysical function would facilitate the assessment of critical surfactant alterations in the perspective of the pathophysiology of these different diseases. The majority of studies investigating the manner in which surfactant is compromised in pulmonary conditions utilize small animal models of lung disease; thus, an understanding of surfactant's structure-function relationship in laboratory animals such as the rat is required [8–11].

Surfactant is composed of 90–95% lipids and 5–10% surfactant-associated proteins and is relatively conserved among mammalian species [12]. The active form of surfactant, the large aggregates (LA), is isolated from lung lavage by differential centrifugation. Isolated LA reduce surface tension values to near 0 mN/m in vitro and can restore lung function in surfactant-deficient animals [13]. LA contain ~70% phosphatidylcholine (PC), ~10% phosphatidylglycerol (PG), ~8% cholesterol, ~10% surfactant associated proteins (designated SP-A, SP-B and SP-C), and low levels of other lipids [14]. Further analysis of the major lipid, PC, from different animal species has revealed a characteristic molecular species profile, including 40–60% of the disaturated species, dipalmitoyl-PC (DPPC) [15].

To accomplish its function, surfactant forms a lipid-rich surface film at the air-liquid interface, which, upon compression, reduces surface tension to very low values [12]. Based on the high levels of disaturated phospholipids within surfactant, which by themselves can reduce surface tension to low values upon compression, the original mechanistic theory of surfactant function was that surfactant reduces

* Corresponding author at: Lawson Health Research Institute, Room E4-146, 268 Grosvenor Street, London, ON, Canada N6A 4V2. Tel.: +1 519 646 6100x64092; fax: +1 519 646 6110.
E-mail address: rveldhui@uwo.ca (R.A.W. Veldhuizen).

0301-4622/$ – see front matter © 2011 Elsevier B.V. All rights reserved.
doi:10.1016/j.bpc.2011.06.001

alveolar surface tension by forming a monolayer of surfactant lipids and subsequently enriching this film in disaturated lipids [12]. This theory of a compositional alteration of the surface film has recently been challenged [16,17]. One alternative theory is that a structural rearrangement of surface components provides the crucial aspect in surface tension reduction [2,18]. The majority of evidence for this alternative mechanism stems from studies utilizing reconstituted and exogenous surfactants. Data on surface film structures of endogenous surfactant preparations is limited and is important to elucidate in order to fully understand the complex biophysical behavior of this lipoprotein mixture.

Therefore, the objective of our study was to characterize the surface film structure obtained from isolated LA from normal adult rats. Specifically, we utilized Atomic Force Microscopy (AFM) to detect height differences between various regions of a surfactant film at different surface pressures. These height differences are due to the orientation and packing of the lipids within the surface film and allow for the differentiation of the fluid liquid-expanded (LE) phase, the less fluid liquid-ordered (LO) phase and the solid liquid-condensed (LC) phase [2]. In addition, AFM will detect height differences due to the presence of stacks of phospholipid bilayers.

2. Material and methods

2.1. Rat surfactant isolation

All procedures were approved by the animal use subcommittee at the University of Western Ontario under the guidelines of the Canadian Council of Animal Care. A total of 11 male Sprague–Dawley rats (350 g to 450 g) were killed with intravenous administration of an overdose of pentobarbital sodium after which an endotracheal tube was inserted. The lung was lavaged through the endotracheal tube with 10 ml of sterile 0.15 M NaCl solution, which was instilled and withdrawn three times. Five separate lavages were performed and the combined volume was recorded. The total lavage was centrifuged at 150×*g* for 10 min to eliminate the cell debris to obtain total surfactant which was further centrifuged at 40,000×*g* for 15 min to separate the large aggregates (LA) pellet subfraction from the supernatant small aggregates (SA) subfraction [13]. The LA subfraction was subsequently resuspended in 2 ml of sterile 0.15 M saline and stored at −20 °C.

2.2. Sample preparation

The rat LA samples were extracted according to the method of Bligh and Dyer using chloroform:methanol (2:1 v/v) [19]. The chloroform phase, which contains the hydrophobic surfactant components, was dried under nitrogen gas followed by the reconstitution of the dried samples in chloroform which contains ethanol as a preservative. The aliquots were taken to determine the phospholipid concentration of each extracted sample by Duck–Chong phosphorus assay [20]. The remaining extracted LA was then dried in nitrogen gas and stored at −20 °C for the following biophysical studies.

Acetone precipitation, to remove cholesterol, was performed on the combined extract of 6 animals [21]. An aliquot of this pooled extract was dissolved in chloroform and shell-dried inside a test tube. Two milliliters of pre-chilled acetone, covering the entire lipid film, was used to extract cholesterol at −20 °C for 48 h. Subsequently, the sample was centrifuged at 250×*g* for 10 min and the acetone fraction was decanted. The remaining film was dried and resuspended in chloroform/methanol and aliquots were taken to determine the phospholipid concentration of the sample by the Duck–Chong phosphorous assay [20] and cholesterol concentration using a commercially available free cholesterol kit (Free Cholesterol E, Wako Chemicals, Richmond, VA). The remaining acetone precipitated LA was then dried under nitrogen and stored at −20 °C for further analyses. Preliminary studies using BLES (bovine lipid extract surfactant) demonstrated that over 95% of the phospholipids-phosphorous was recovered following this procedure.

Similar procedures of extraction and phosphorus and cholesterol measurements were performed on the exogenous surfactant preparation BLES, which was a kind gift from BLES Biochemicals (London ON, Canada).

2.3. Langmuir surface balance

Preparation of solid supported surfactant films was carried out using a Langmuir balance (μ-trough, Kibron Inc. Helsinki, Finland) at room temperature (24 °C ± 1 °C). A detailed description of the experimental setup and procedures can be found elsewhere [18]. Briefly, the extracted samples from each group were reconstituted in chloroform at a concentration of 1 mg phospholipid per ml. The solutions were applied drop-wise using a micro-syringe on freshly prepared Millipore deionized distilled water (≥18.2 MΩ-cm) (Milli-Q quality, Millipore, Billerica, MA) in the polytetrafluoethylene (PTFE) trough of the Langmuir balance to form a monolayer film. After 15 min, which allowed the chloroform to evaporate, the films were compressed by a continuous PTFE ribbon at a rate of 8 Å2/chain/s and the surface pressure was continuously monitored and recorded by a Wilhelmy plate to generate the surface pressure (π)-area (A) isotherms. Note that the recorded data represents surface pressure, which is defined as the surface tension of the clean surface minus the surface tension of the sample [22]. The films were deposited on previously submerged mica, which was cleaned by multiple exfoliations, by lifting it up from the water phase at constant surface pressures of 10 mN/m, 20 mN/m, 30 mN/m, 40 mN/m or 50 mN/m, using a rate of 2 mm/min that resulted in a transfer ratio of 1.

2.4. Film imaging by AFM

A MultiMode™ scanning probe microscope (MM-SPM) (Digital Instruments, Veeco Metrology Group, Group, Santa Barbara) was used to study the structures of the surfactant films in air. The films were scanned with a J-type scanner using contact mode for the films obtained at pressure 10–40 mN/m and, based on preliminary experiments and to avoid damage to the surface film, in tapping mode for the films at 50 mN/m. A silicon nitride cantilever with a spring constant of 0.12 N/m was used for contact mode imaging and a silicon probe with fo = 301–365 kHz was used for tapping mode imaging. The images were analyzed using Nanoscope 5.30r3sr3 and ImageJ (NIH). Different regions of each sample were imaged at various magnifications. All images were taken at the resolution of 512×512 pixels. Specific height-phase correlations were based on previous studies using lipid mixtures and exogenous surfactants [2,23,24].

2.5. Phospholipid profile determination: electrospray ionization mass spectrometry (ESI-MS)

The phospholipid profile of extracted LA samples was analyzed directly by ESI-MS for molecular mass by infusion [25]. The samples were prepared by resuspending extracted LA in chromatographic grade chloroform:methanol (1:3) to a final concentration of 0.5 nmol/μL. The internal standards dimyristoyl-PC and diacetylene-phosphorylcholine were added at a concentration of 0.05 nmol/μL. Thus, the final molarity of the sample was 0.700 nmol/μL. The injection solvent was 70:20:8:2 MeOH: CHCl3: water: NH3 at a flow rate 40 μL/min. Mass spectrometry was performed on a triple quadrupole mass spectrometer (Micromass, Beverly, MA, USA) equipped with a Z-spray source to analyze the PC species. Calibration was performed with NaI. MassLynx 4.0 (Micromass, Manchester, England) software was used to acquire the data. The phospholipid profiles were expressed as the mole percentage of individual PC

molecular species which were identified by their specific molecular weight.

2.6. Data analysis

AFM images were analyzed using Nanoscope 5.30r3sr3 for height analysis and ImageJ for area analysis. The data for each group were based on the measurements from at least 3 samples. Each sample was analyzed at 3 resolutions: 50 μm × 50 μm, 20 μm × 20 μm, 10 μm × 10 μm. All values reported from all the experiments are expressed as mean ± standard error (SE). Comparisons between different surface pressures, as well as comparisons among the three different experimental groups, were analyzed by one-way analysis of variance (ANOVA) followed by Tukey's post hoc test. The statistical software utilized was Graphpad Prism and p values less than 0.05 were considered significant.

3. Results

All animals were utilized to obtain surfactant LA for surface film analysis. In addition, four animals underwent a pressure volume curve analyses and their lavages were analyzed for surfactant pool size information to reflect the baseline characteristics of these animals. On average the volume of air inflated into the lungs of these animals at the maximum pressure of 26 cmH_2O during the pressure volume curve analysis was 33.1 ± 2.3 ml/kg. The amount of surfactant recovered in the lavage from these animals was 4.5 ± 0.3 mg phospholipids/kg consisting of 2.3 ± 0.2 mg/kg LA, with the remainder being SA.

Chloroform extracted LA samples, containing the hydrophobic surfactant components consisting of phospholipids, cholesterol and the surfactant associated proteins SP-B and SP-C, were utilized to obtain Surface Pressure–Relative Surface Area (π-A) compression isotherms. Fig. 1 shows such isotherms from 3 individual animals. Samples were spread on the water surface up to a surface pressure just below 10 mN/m and during subsequent compression, the surface pressure increased (i.e. the surface tension decreased) as a function of the reduction in surface area. At the start of surface area reduction, the surface pressure increased rapidly in response to the compression. At a pressure of approximately 40 mN/m a plateau was observed in which changes in area only led to a slight increase in surface pressure. Subsequent to this plateau, surface pressure once again increased more rapidly with a decrease in surface area. These features were consistently observed for all three individual samples.

In order to study the structural correlates to these changes in surface pressures up to the plateau pressure, surface film samples were deposited on mica at surface pressures 10, 20, 30, 40 mN/m and analyzed by AFM. Typical AFM images, at two different magnifications, are shown in Fig. 2 with height quantification results of the images shown in Table 1. Overall, the images of the rat LA films exhibit coexistence of several phases. At surface pressures 10, 20 and 30 mN, several different structural features are observed. Based on the current literature, the darker (lower) region can be assumed to be the more fluid liquid-expanded (LE) phase [26]. Scattered within this LE phase are micrometer-sized domains that are approximately 0.7 nm higher than the LE phase, indicative of the less fluid liquid-ordered (LO) phase as previously described [2,23,24]. Within these micro-domains are areas of higher regions, termed domains-within-domains, which are approximately 1.1 nm above the LE phase suggesting they represent the liquid-condensed (LC) phase. In addition, there are nanometer size domains within the LE phase which, based on their height are also reflective of the LC phase. Whereas these three phases are consistently observed up to a surface pressure of 30 mN/m, only LE and LC phases were observed in the samples analyzed at 40 mN/m.

Quantification of the size and area covered by micro-domains, and area covered by nano-domains, is shown in Table 2. The average size of the micro-domains was not significantly different among the different surface pressures and was in the range of 10–25 μm^2. The

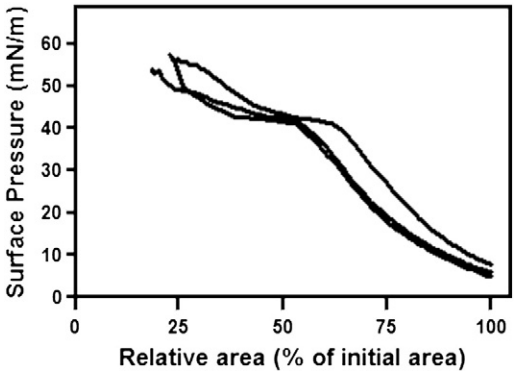

Fig. 1. Surface pressure-relative area (fraction of initial area) (π-A) compression isotherms were prepared from three individual samples obtained from normal Sprague–Dawley rats.

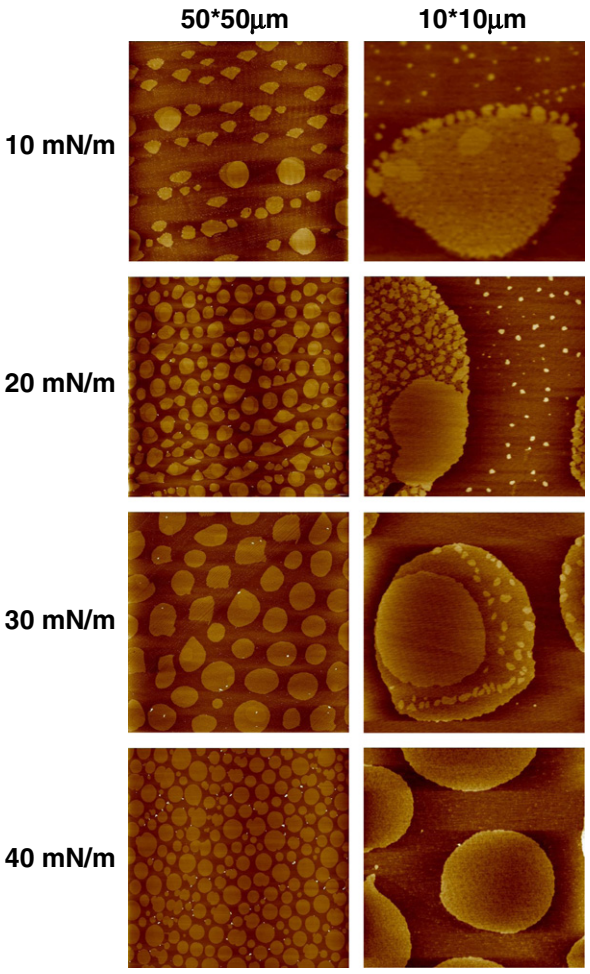

Fig. 2. Representative AFM images of the normal rat LA samples. The images were obtained at different surface pressures varying from 10 to 40 mN/m as indicated on the figure. The left panel represent images of 50 μm × 50 μm, and the right panel are of 10 μm × 10 μm. Higher areas are indicated by lighter colors.

Table 1
Height differences of micro and nano-domains of normal rat LA at different surface pressures.

Height (nm) relative to liquid-expanded phase			
Surface pressure (mN/m)	Micro-domains	Domain-within-Domain	Nano-domains
10	0.57 ± 0.057	1.1 ± 0.04	1.3 ± 0.08
20	0.72 ± 0.048	1.1 ± 0.08	0.98 ± 0.11
30	0.82 ± 0.039	1.1 ± 0.03	1.2 ± 0.17
40	1.19 ± 0.132	NA	NA

Average ± SEM, n = 3 animals/group with multiple images analyzed for each animal. NA = not applicable.

Table 2
Size and area covered by domain structures of normal rat LA at different surface pressures.

Surface pressure (mN/m)	Micro-domains size (μm2)	Micro-domains area covered (%)	Nano-domains area covered (%)
10	16.1 ± 4.3	27.2 ± 3.3	4.5 ± 0.5
20	10.4 ± 2.1	45.2 ± 1.3*	2.0 ± 0.5*
30	15.5 ± 1.2	44.5 ± 1.5*	2.4 ± 0.3*
40	25.4 ± 6.3	61.8 ± 4.9*#	0.7 ± 0.07*#

Average ± SEM, n = 3 animals/group with multiple images analyzed for each animal. * = $p<0.05$ versus 10 mN/m, # = $p<0.05$ versus 30 mN/m.

area covered by these domains increased with increasing surface pressure, reaching statistical significance at 20 and 30 mN/m compared to 10 mN/m, and at 40 mN/m compared to all other surface pressures. The nano-domains were relatively uniform in size and covered a small percentage of the area at 10 mN/m (4.5%). This area covered by nano-domains decreased significantly with increasing surface pressure such that at 40 mN/m nano-domains covered less than 1% of the surface area (Table 2).

The AFM images obtained at 50 mN/m are shown in Fig. 3. At this pressure, height differences observed within the surface film become much larger than those observed at the lower pressures due to the formation of multilayers. Height analysis indicates that the lighter colored regions are either approximately 4, 8 or 12 nm higher than the surrounding areas, which is reflective of the formation of one, two or three stacks of bilayers.

One of the surprising structural features of our rat surfactant extract was the presence of the domain-within-domain feature at low surface pressures. Such structures were not observed in goat surfactant or BLES [18,27], however those samples contain relatively low levels of cholesterol. In order to test if the levels of cholesterol within rat surfactant were responsible for these domain-within-domain structures, we performed acetone precipitation to lower the cholesterol concentration from 7.4% to 3.3% (w/w%). In order to examine the effect of acetone precipitation on the composition of the major phospholipid species, phosphatidylcholine, compositional analysis by mass spectrometry was performed. A sample of BLES, which contained 3.7% cholesterol was also examined as a control. The results in Table 3 show that there was no significant difference in the molecular species of PC between the acetone precipitated rat LA and the normal rat LA. Interestingly, comparison of the rat surfactant with BLES indicates a significantly higher proportion of disaturated PC species in rat surfactant. The PG species of two acetone precipitated rat LA samples and two of the normal rat LA samples also showed similar profiles but could not be analyzed statistically due to the low n-value (data not shown).

Representative AFM images of normal rat LA, acetone precipitated rat LA and BLES at 20 mN/m are shown in Fig. 4. The images of the rat LA demonstrated the domain-within-domain structures as described above whereas in the images of acetone precipitated rat LA this feature was not present; the samples showed coexistence of only two different liquid phases. The micro-domains of rat LA and acetone precipitated rat LA covered a similar surface area (45.2% ± 1.3 versus 38.9% ± 6.7, $p>0.05$), however, the domain size was significantly larger in the acetone precipitated samples (21.3 μm2 ± 7.8 versus 10.4 μm2 ± 2.1, $p<0.05$) and was significantly higher (1.5 nm ± 0.05 versus 0.7 nm ± 0.05, $p<0.05$). It should also be noted that a number of very bright spots, approx 15 nm in height and usually at the edges of the micro-sized domains, were observed in the acetone precipitated samples; the nature of these spots is unknown. Further, comparison of normal rat LA and acetone precipitated rat LA at different surface pressures is shown in online supplemental Fig. 1. The results show similar patterns as described for surface pressure 20 mN/m. Examination of BLES at 20 mN/m showed the coexistence of two lipid phases, similar to the acetone precipitated samples (Fig. 4). In general, BLES samples contained fewer micro-domains and more nano-domains. The abundance of these structures was not quantified in the current study but has been reported previously [18].

4. Discussion

Since rats are utilized extensively for studies on lung diseases [8–11], and since alterations of surfactant may be a mechanism leading to lung dysfunction [6,28], the objective of our study was to characterize the structural features of normal rat surfactant interfacial films at different surface pressures. Overall, this study demonstrated that rat surfactant films compressed up to 40 mN/m surface pressure showed a lipid film structure with three distinct phases: liquid expanded phase (LE), liquid ordered phase (LO) and liquid condensed phase (LC) [26], with the more solid LC domains increasing in area coverage with increasing surface pressure. The novel finding of the presence of the LO phase within these structures appears to be related to the endogenous levels of cholesterol within the rat surfactant, since reduction of the cholesterol led to the disappearance of this phase. At surface pressure 50 mN/m these domain features were no longer observed and the film appeared to be a single phase, likely LC, with stacks of multilayers. When interpreting this data,

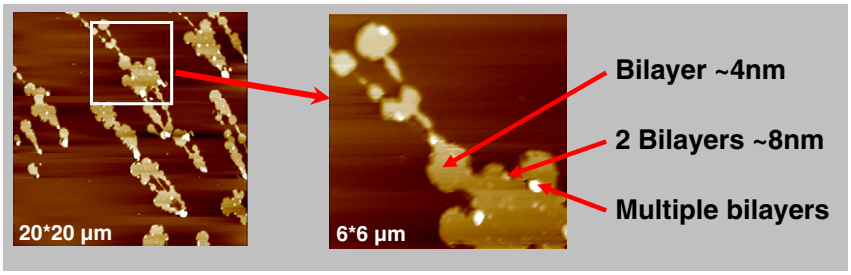

Fig. 3. Representative AFM images of the normal rat LA samples at 50 mN/m. Images at 20 μm × 20 μm and 6 μm × 6 μm are shown with arrows indicating height differences corresponding to one and multiple bilayers.

Table 3
Phosphatidylcholine profiles from BLES, the normal Rat LA and Acetone precipitated Rat LA.

Mass	Species	BLES	Normal	Acetone precipitated
706	PC16:0/14:0	8.38 ± 0.08	13.84 ± 0.26*	14.35 ± 0.78*
730	PC14:0/18:2	0.49 ± 0.08	0.48 ± 0.10	0.60 ± 0.40
732	PC16:0/16:1	12.49 ± 0.20	9.21 ± 0.43	12.80 ± 4.67
734	PC16:0/16:0	38.97 ± 1.15	58.50 ± 0.74*	58.39 ± 8.55
756	PC16:1/18:2	0.15 ± 0.07	0.19 ± 0.11	0.23 ± 0.19
758	PC16:0/18:2	5.18 ± 0.19	3.01 ± 0.23	3.80 ± 1.57
760	PC16:0/18:1	24.36 ± 0.66	3.21 ± 0.59*	4.47 ± 1.27
762	PC16:0/18:0	3.34 ± 0.25	3.67 ± 0.39	2.53 ± 0.18
778	PC14:0/22:6	0.02 ± 0.02	0.12 ± 0.06	0.01 ± 0.01
780	PC16:1/20:4	0.08 ± 0.02	0.13 ± 0.03	0.09 ± 0.08
782	PC16:0/20:4	0.43 ± 0.05	1.12 ± 0.29	0.56 ± 0.26
784	PC18:1/18:2	0.92 ± 0.13	0.80 ± 0.16	0.22 ± 0.20
786	PC18:0/18:2	2.69 ± 0.20	0.52 ± 0.21*	0.34 ± 0.22*
788	PC18:0/18:1	1.29 ± 0.07	0.66 ± 0.20	0.22 ± 0.15*
790	PC18:0/18:0	0.33 ± 0.08	0.37 ± 0.07	0.45 ± 0.25
806	PC16:0/22:6	0.09 ± 0.06	1.06 ± 0.33	0.14 ± 0.06
808	PC18:1/20:4	0.23 ± 0.06	0.08 ± 0.05	0.07 ± 0.02
810	PC18:0/20:4	0.25 ± 0.04	0.24 ± 0.14	0.17 ± 0.10
812	PC18:0/20:3	0.12 ± 0.04	1.54 ± 0.19	0.27 ± 0.05
814	PC18:0/20:2	0.04 ± 0.03	0.72 ± 0.18	0.10 ± 0.06
816	PC18:0/20:1	0.04 ± 0.02	0.36 ± 0.13	0.09 ± 0.05
818	PC18:0/20:0	0.10 ± 0.03	0.17 ± 0.01	0.11 ± 0.04

Data are presented as molar percentage of PC species. Values are an average of three measurements and are expressed as mean ± SE. * = $p<0.05$ compared to BLES.

it should be noted that due to the restriction of the mechanical design of the Langmuir balance, the surfactant film could not be compressed to higher surface pressures, and the rate at which the film was compressed is relatively low. In addition, all of the films were prepared at room temperature on the surface of a water subphase and deposited on mica, both of which may influence the behavior of these films [29].

Compression of rat surfactant lipid extracts on the Langmuir–Wilhelmy surface balance resulted in increased surface pressures to approximately (~40 mN/m), followed by a plateau at which compressions only resulted in small increases in surface pressure. It has previously been shown that following this plateau is a more rapid increase in surface pressure to values thought necessary to stabilize the lung [2,12]. Previous studies have investigated the phase behavior of these types of films using fluorescence microscopy [30,31]. In the current study the physical/structural events occurring within the surface pressure-area isotherms were clarified by AFM. This method provides information on phase separation based on height differences within the film, with a higher resolution than fluorescence microscopy and without inclusion of external probes. AFM also allows the detection of multilayer formation. Specific height-phase correlations have been characterized using lipid mixtures [2,23,24]. The AFM images of rat surfactant demonstrated a general progression of phase separation and domain formation at low surface pressure, increases in the surface area covered by domains with increased surface pressure, and finally bilayer/multilayer formation during the plateau of the surface pressure area isotherm. Together with previous studies [18,27], these results support the overall concept that in order to reduce surface tension surfactant forms distinct lipid domains enriched in disaturated lipids that upon further compression lead to the exclusion of lipid bilayers from the surface film which may reinsert upon expansion. Beyond the support for the general concept, rat surfactant also provided several distinct structural characteristics which will be further discussed below.

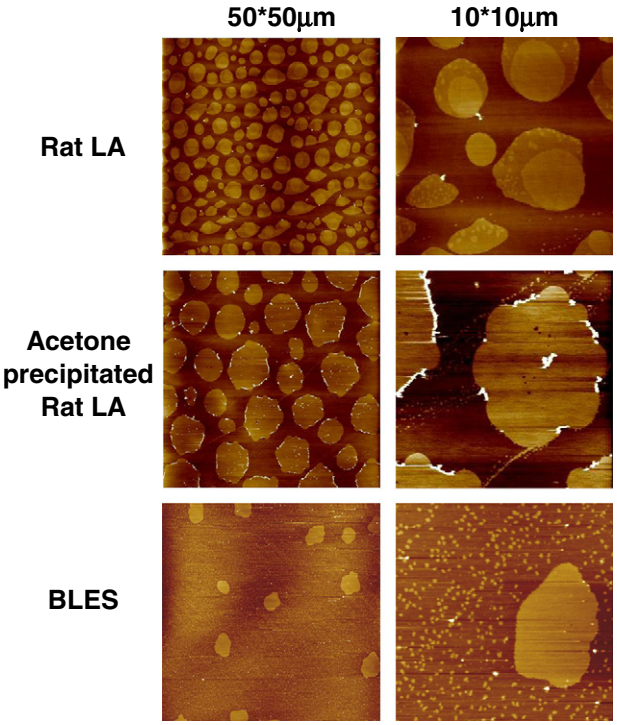

Fig. 4. Representative AFM images of the normal rat LA sample, acetone-precipitated rat LA and BLES at 20 mN/m. Images at 50 μm × 50 μm and 10 μm × 10 μm are shown.

While a number of previous studies have provided insight into surfactant film structure via AFM and other techniques based on reconstitution of the major lipids and proteins of surfactant [23,32,33], we have focused on the compositionally more complex situation of chloroform-extracted endogenous surfactant. In this specific area of investigation, the majority of studies have been performed on animal derived exogenous surfactant preparations such as the bovine preparation, BLES, and the porcine derived surfactant, Curosurf [18,34–36]. A thorough AFM examination of the surface film structure of BLES and several other clinical surfactant preparations at different surface pressures has been reported [18,36]. Due to their clinical purpose, isolation and processing of such preparations is quite different than those used to simply isolate endogenous surfactant from a rat. For example, Survanta and Curosurf are produced from minced lung extracts which have been supplemented with DPPC and other components. The bovine preparations, Calfactant and BLES, are exogenous preparations made from lavage material and are more closely related to the rat surfactant since they also contain the complex surfactant lipid profile and the hydrophobic surfactant proteins SP-B and SP-C. Comparisons of the rat surfactant films and the reported structures of the most thoroughly analyzed exogenous surfactant, BLES, at pressures up to 40 mN/m indicate marked differences. The first difference was that the present study demonstrated an increase in area covered by micro-domains with increasing surface pressure up to 40 mN/m, whereas BLES samples exhibited a decrease in micro-domains with a corresponding increase in nano-domains with increasing pressure [18,36]. In spite of the apparent difference in the relative percentage of the micrometered and nanometered LC domains, the total area covered by LC domains in rat surfactant is consistent with the portion of disaturated phospholipid. As shown in Table 2, at 40 mN/m, approximately 60% surface monolayer was covered by LC domains. This percentage is likely related to the percentage of disaturated phospholipids in the surfactant. As such, the high percentage of area covered for rat surfactant is consistent with it containing 58.5 ± 0.74% DPPC (Table 3) whereas BLES, which contains ~40% DPPC, had ~40% of its surface monolayer covered by LC domains (both micro-domains and nano-domains) at 40 mN/m [18]. These findings consistently suggest that selective film refining does not occur at the interfacial monolayer, at least up to a moderately high surface pressure of 40 mN/m [2,18]. The comparison of chemical composition and film organization between BLES and rat surfactant

also suggests that the formation of micro-domains and nano-domains, and the conversion from one into another, within the surfactant monolayers is a much more complicated process than previous suggestions of it being only affected by surface pressure and cholesterol [18,36–38]. The specific phospholipid profile (relative percentage of saturated and unsaturated phospholipids) and the level of surfactant proteins may also contribute to the micro and nano domain formation within the surfactant monolayer.

The second distinct structural feature observed in the rat samples but not in BLES, was the domain-within-domain structure observed at low surface pressures. The height differences suggest that these domains-within-domains represent areas of LC phase within a lipid domain in the LO phase. The progression over different surface pressures indicates that the LO phase micro-domains become more ordered leading to a LC phase without domains-within-domains at 40 mN/m, immediately prior to the plateau pressure. We relate this unique domain-in-domain feature to the cholesterol levels present in rat surfactant based on two lines of evidence. First, a previous study from our group has demonstrated that the addition of a non-physiological amount of cholesterol to BLES resulted in domain-within-domain structures [39]. Second, reduction of the cholesterol from rat surfactant by approximately 50%, without changing the phosphatidylcholine profile, resulted in disappearance of the domain-in-domain feature. Elevated cholesterol has recently been implicated with impaired surfactant function [40,41]. Studies by the Amrein group led to the suggestion that high cholesterol levels inhibit surfactant by preventing the monolayer to multilayer transition [42]. Furthermore, the domain-within-domain feature was previously only observed at cholesterol levels above the normal physiological levels [39]. In the current study, the amount of cholesterol simply represented the amount endogenously present within this surfactant, and was associated with the domain-within-domain features and multilayer formation. The conclusion that can be made from these observations is that this domain-within-domain feature itself is not directly responsible for surfactant inhibition by cholesterol.

To our knowledge, only one other study on endogenous surfactant has been reported [27]. Surfactant LA were isolated from goat lavage fluid and the extracts of these LA were analyzed for composition and structure by AFM. Surprisingly, the goat surfactant had only 0.6% cholesterol, by far the lowest levels of cholesterol reported for a mammalian species. Since the study did not analyze the domain structures and height quantitatively and/or statistically, detailed comparisons with rat surfactant are difficult to make. However, the representative images shown had some interesting features compared to rat surfactant. For example, the authors reported the presence of circular domains up to a surface pressure of 20 mN/m, but above these pressures the domains no longer remained round, whereas rat surfactant samples showed generally round domains. The authors suggested these shapes were the result of reduced line tension at the edges of the domain as a consequence of the low cholesterol values, although it should be noted that the relation between line tension, cholesterol levels and surface pressure is complex [38]. Another difference with our rat LA films was that no domains-within-domains were observed within the goat surfactant films, which, considering the low levels of cholesterol, is consistent with our interpretation of the role of cholesterol in the formation of these structures.

In conclusion, analysis of the structural features of rat surfactant by AFM led to phase separation at low surface pressures and multilayer formation at higher surface pressure. At low pressures we observed a novel domain-within-domain feature which was related to cholesterol levels. Previous reports demonstrated phase separation at the lower pressures, however the shape, size and/or area covered by these domains is different among different preparations. These results imply that the presence of a sufficient area of LC domains of lipid within the film, but not the size and shape of these domains, is sufficient for monolayer-to-multilayer transition and that multilayer formation represents the critical functional process at high surface pressures among the surfactant from different sources. In addition, the structural analysis of rat surfactant may provide a reference point for other studies to investigate the structural correlates of surfactant dysfunction in models of ALI and other pulmonary diseases.

Supplementary materials related to this article can be found online at doi:10.1016/j.bpc.2011.06.001.

Acknowledgments

The authors thank Lynda McCaig, Dr. Suya Liu and Dr. Li-Juan Yao for technical assistance, Jesse Lewis, Lakshman Vasanthamohan and Joshua Qua Hiansen for proofreading the manuscript and Drs. Cory Yamashita, Nils Petersen and Jim Lewis for helpful discussions. These studies were supported by funding from the Canadian Institutes of Health Research and the Ontario Thoracic Society.

References

[1] L.M.G. Van Golde, J.J. Batenburg, B. Robertson, The pulmonary surfactant system, News Physiol. Sci. 9 (1994) 13–20.
[2] Y.Y. Zuo, R.A. Veldhuizen, A.W. Neumann, N.O. Petersen, F. Possmayer, Current perspectives in pulmonary surfactant — inhibition, enhancement and evaluation, Biochim. Biophys. Acta 1778 (2008) 1947–1977.
[3] B. Robertson, Background to neonatal respiratory distress syndrome and treatment with exogenous surfactant, Dev. Pharmacol. Ther. 13 (1989) 159–163.
[4] A.A. Maruscak, D.W. Vockeroth, B. Girardi, T. Sheikh, F. Possmayer, J.F. Lewis, R.A. Veldhuizen, Alterations to surfactant precede physiological deterioration during high tidal volume ventilation, Am. J. Physiol. Lung Cell. Mol. Physiol. 294 (2008) L974–L983.
[5] A. Gunther, M. Balser, R. Schmidt, P. Markart, A. Olk, J. Borgermann, F.H. Splittgerber, W. Seeger, I. Friedrich, Surfactant abnormalities after single lung transplantation in dogs: impact of bronchoscopic surfactant administration, J. Thorac. Cardiovasc. Surg. 127 (2004) 344–354.
[6] R.A. Veldhuizen, L.A. McCaig, T. Akino, J.F. Lewis, Pulmonary surfactant subfractions in patients with the acute respiratory distress syndrome, Am. J. Respir. Crit. Care Med. 152 (1995) 1867–1871.
[7] M. Griese, Pulmonary surfactant in health and human lung diseases: state of the art, Eur. Respir. J. 13 (1999) 1455–1476.
[8] T.C. Bailey, A.A. Maruscak, E.L. Martin, A.R. Forbes, A. Petersen, L.A. McCaig, L.J. Yao, J.F. Lewis, R.A. Veldhuizen, The effects of long-term conventional mechanical ventilation on the lungs of adult rats, Crit. Care Med. 36 (2008) 2381–2387.
[9] T. Tschernig, D. Neumann, A. Pich, M. Dorsch, R. Pabst, Experimental bronchial asthma — the strength of the species rat, Curr. Drug Targets 9 (2008) 466–469.
[10] A.J. Aspros, C.G. Coto, J.F. Lewis, R.A. Veldhuizen, High-frequency oscillation and surfactant treatment in an acid aspiration model, Can. J. Physiol. Pharmacol. 88 (2010) 14–20.
[11] M. de Perrot, S.M. Quadri, Y. Imai, S. Keshavjee, Independent ventilation of the graft and native lungs in vivo after rat lung transplantation, Ann. Thorac. Surg. 79 (2005) 2169–2171.
[12] J. Goerke, Pulmonary surfactant: functions and molecular composition, Biochim. Biophys. Acta 1408 (1998) 79–89.
[13] A.M. Brackenbury, J.L. Malloy, L.A. McCaig, L.J. Yao, R.A. Veldhuizen, J.F. Lewis, Evaluation of alveolar surfactant aggregates in vitro and in vivo, Eur. Respir. J. 19 (2002) 41–46.
[14] R.A.W. Veldhuizen, K. Nag, S. Orgeig, F. Possmayer, The role of lipids in pulmonary surfactant, Biochim. Biophys. Acta 1408 (1998) 90–108.
[15] A.D. Postle, E.L. Heeley, D.C. Wilton, A comparison of the molecular species compositions of mammalian lung surfactant phospholipids, Comp. Biochem. Physiol. A Mol. Integr. Physiol. 129 (2001) 65–73.
[16] S. Rugonyi, S.C. Biswas, S.B. Hall, The biophysical function of pulmonary surfactant, Respir. Physiol. Neurobiol. 163 (2008) 244–255.
[17] B. Piknova, W.R. Schief, V. Vogel, B.M. Discher, S.B. Hall, Discrepancy between phase behavior of lung surfactant phospholipids and the classical model of surfactant function, Biophys. J. 81 (2001) 2172–2180.
[18] Y.Y. Zuo, E. Keating, L. Zhao, S.M. Tadayyon, R.A. Veldhuizen, N.O. Petersen, F. Possmayer, Atomic force microscopy studies of functional and dysfunctional pulmonary surfactant films. I. Micro- and nanostructures of functional pulmonary surfactant films and the effect of SP-A, Biophys. J. 94 (2008) 3549–3564.
[19] E.G. Bligh, W.J. Dyer, A rapid method of total lipid extraction and purification, Can. J. Biochem. Physiol. 37 (1959) 911–917.
[20] C.G. Duck-Chong, A rapid sensitive method for determining phospholipid phosphorus involving digestion with magnesium nitrate, Lipids 14 (1979) 492–497.
[21] D.S. Woodard, K.K. Ostrom, L.M. McManus, Lipid inhibitors of platelet-activating factor (PAF) in normal human plasma, J. Lipid Mediators Cell Signal. 12 (1995) 11–28.
[22] G.L. Gaines, Insoluble Monolayers at Liquid–Gas Interfaces, John Wiley & Sons, New York, 1966.

[23] R.V. Diemel, M.M. Snel, L.M. Van Golde, G. Putz, H.P. Haagsman, J.J. Batenburg, Effects of cholesterol on surface activity and surface topography of spread surfactant films, Biochemistry (N. Y.) 41 (2002) 15007–15016.
[24] L. Wang, P. Cai, H.J. Galla, H. He, C.R. Flach, R. Mendelsohn, Monolayer-multilayer transitions in a lung surfactant model: IR reflection-absorption spectroscopy and atomic force microscopy, Eur. Biophys. J. 34 (2005) 243–254.
[25] K. Rodriguez-Capote, D. Manzanares, T. Haines, F. Possmayer, Reactive oxygen species inactivation of surfactant involves structural and functional alterations to surfactant proteins SP-B and SP-C, Biophys. J. 90 (2006) 2808–2821.
[26] J. Perez-Gil, Structure of pulmonary surfactant membranes and films: the role of proteins and lipid-protein interactions, Biochim. Biophys. Acta 1778 (2008) 1676–1695.
[27] S. Mukherjee, K. Maiti, M. Fritzen-Garcia, S.C. Bhattacharya, K. Nag, A.K. Panda, S.P. Moulik, Physicochemical studies on goat pulmonary surfactant, Biophys. Chem. 134 (2007) 1–9.
[28] I. Frerking, A. Gunther, W. Seeger, U. Pison, Pulmonary surfactant: functions, abnormalities and therapeutic options, Intensive Care Med. 27 (2001) 1699–1717.
[29] J. Yang, J. Appleyard, The main phase transition of mica-supported phosphatidylcholine membranes, J. Phys. Chem. B 104 (2000) 8097–8100.
[30] K. Nag, J. Perez-Gil, M.L. Ruano, L.A. Worthman, J. Stewart, C. Casals, K.M. Keough, Phase transitions in films of lung surfactant at the air–water interface, Biophys. J. 74 (1998) 2983–2995.
[31] B.M. Discher, W.R. Schief, V. Vogel, S.B. Hall, Phase separation in monolayers of pulmonary surfactant phospholipids at the air-water interface: composition and structure, Biophys. J. 77 (1999) 2051–2061.
[32] M.T. Dohm, N.J. Brown, S.L. Seurynck-Servoss, la S de, A.E. Barron, Mimicking SP-C palmitoylation on a peptoid-based SP-B analogue markedly improves surface activity, Biochim. Biophys. Acta 1798 (2010) 1663–1678.
[33] K. Nag, S.G. Taneva, J. Perez-Gil, A. Cruz, K.M. Keough, Combinations of fluorescently labeled pulmonary surfactant proteins SP-B and SP-C in phospholipid films, Biophys. J. 72 (1997) 2638–2650.
[34] Z. Leonenko, E. Finot, V. Vassiliev, M. Amrein, Effect of cholesterol on the physical properties of pulmonary surfactant films: atomic force measurements study, Ultramicroscopy 106 (2006) 687–694.
[35] P.C. Stenger, C. Alonso, J.A. Zasadzinski, A.J. Waring, C.L. Jung, K.E. Pinkerton, Environmental tobacco smoke effects on lung surfactant film organization, Biochim. Biophys. Acta 1788 (2009) 358–370.
[36] H. Zhang, Q. Fan, Y.E. Wang, C.R. Neal, Y.Y. Zuo, Comparative study of clinical pulmonary surfactants using atomic force microscopy, Biochim. Biophys. Acta 1808 (2011) 1832–1842.
[37] B.M. Discher, K.M. Maloney, D.W. Grainger, C.A. Sousa, S.B. Hall, Neutral lipids induce critical behavior in interfacial monolayers of pulmonary surfactant, Biochemistry (N. Y.) 38 (1999) 374–383.
[38] B.M. Discher, K.M. Maloney, D.W. Grainger, S.B. Hall, Effect of neutral lipids on coexisting phases in monolayers of pulmonary surfactant, Biophys. Chem. 101–102 (2002) 333–345.
[39] E. Keating, L. Rahman, J. Francis, A. Petersen, F. Possmayer, R. Veldhuizen, N.O. Petersen, Effect of cholesterol on the biophysical and physiological properties of a clinical pulmonary surfactant, Biophys. J. 93 (2007) 1391–1401.
[40] L. Gunasekara, S. Schurch, W.M. Schoel, K. Nag, Z. Leonenko, M. Haufs, M. Amrein, Pulmonary surfactant function is abolished by an elevated proportion of cholesterol, Biochim. Biophys. Acta 1737 (2005) 27–35.
[41] D. Vockeroth, L. Gunasekara, M. Amrein, F. Possmayer, J.F. Lewis, R.A. Veldhuizen, The role of cholesterol in the biophysical dysfunction of surfactant in ventilator induced lung injury, Am. J. Physiol. Lung Cell. Mol. Physiol. 298 (2010) L117–L125.
[42] Z. Leonenko, S. Gill, S. Baoukina, L. Monticelli, J. Doehner, L. Gunasekara, F. Felderer, M. Rodenstein, L.M. Eng, M. Amrein, An elevated level of cholesterol impairs self-assembly of pulmonary surfactant into a functional film, Biophys. J. 93 (2007) 674–683.